

MODELING GROUNDWATER FLOW THROUGH DIKES FOR REAL TIME STABILITY ASSESSMENT

John M. van Esch

Deltares
Department of geo-engineering
Stieltjesweg 2, Delft, The Netherlands
e-mail: john.vanesch@deltares.nl, web page: <http://www.deltares.nl/>

Key words: Groundwater modeling, real time predictions

Summary. This paper assesses the stability of flood defense systems by dynamic system simulation. Time dependent hydraulic measurements and predictions provide input signals to the dynamic system. A computationally efficient finite volume model based on the Dupuit approximation simulates groundwater flow through the aquifers and aquitards within the system and the embankment itself. Special boundary conditions capture the two-dimensional flow behavior through the flood defense system. Novel measurement techniques monitor the geo-hydrologic system behavior, provide data for calibration of the deterministic model and will support a stochastic real time correction. Bishops method assesses geo-mechanical stability and returns a stability factor, which forms the output signal of the dynamic system. For actual situations the stability response will be simulated for a series of flood water level scenarios and the results advise on maintenance, remediation and adaptation measurements.

1 Introduction

Delft-FEWS⁶ is acknowledged worldwide for the real time forecasting of hydrodynamic water levels and waves in rivers, lakes and seas, using prediction models and monitoring data. This paper presents a new capability of Delft-FEWS, for the coupled real time forecasting of internal heads in dike cross sections, followed by forecasts of the associated slope stability.

Groundwater flow simulations provide predictions of the water pressure field in the dike, which can be used for the stability assessment. The finite element method is often preferred for solving these problems because of the flexibility of this technique in capturing complex geometries¹. However for real time stability assessment calculations the speed is often too slow. The Dupuit assumption² provides an alternative for complex computations. This approximation states that groundwater flow in aquifers is oriented horizontally and flow through aquitards takes place in the vertical direction. Special boundary conditions have to be added to model the two-dimensional flow in the dike. A groundwater

flow simulation predicts the piezometric heads in the aquifers that can be interpolated throughout the flow domain. Piezometric head measurements in a dike section, which is loaded by variable water level conditions, can be used for inverse modeling. Figure 1 illustrates the outcome of a simulation for a system of a single aquifer confined by an aquitard and a dike. The figure shows the piezolines in the aquifer and the embankment and the total stress and water pressure along three vertical lines. The difference between the total stress and water pressure gives the effective stress, which relates to the shear stress and slope stability.

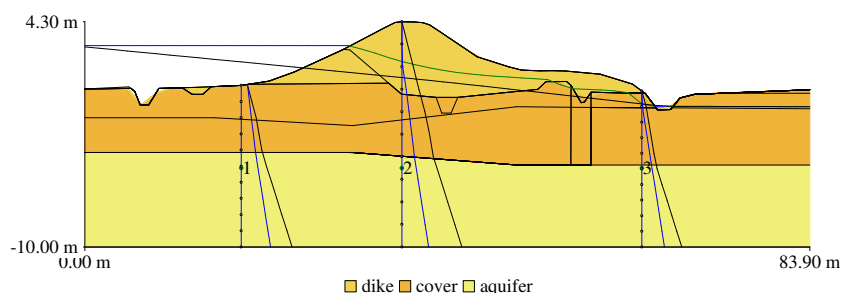


Figure 1: Piezolines and pore pressure.

Slope stability approximations often assume that the soil fails along a circular slip surface for which a stability factor can be calculated⁵. The stability factor compares the actual shear stress at a circular slip surface to the maximum shear stress. Both the actual and maximum shear stress may be calculated numerically, by subdividing the slip circle in slices that are bounded by vertical interfaces. The critical circle follows from solving an optimization problem. Figure 2 shows the critical slip surface, which followed from the evaluation of 1000 circles. A grid of 10×10 points specified the circle center points, and each point considered 10 circle diameters. This optimization problem needs to be solved for each time step.

Section 2 presents the groundwater flow model based on the Dupuit approximation and compares the result of the simplified approach to a fully two-dimensional computation. The coupled groundwater flow - slope stability model is applied in Section 3. Section 4 presents the conclusions. Throughout this paper index notation will be used. Equations are given for Cartesian coordinates x_i (m) and time is denoted by t (s). The domain of interest Ω is enclosed by its boundary Γ .

2 Groundwater flow

Laminar flow through porous media can effectively be modeled by imposing Darcy's law and considering conservation of mass. Darcy's law gives an expression for the specific

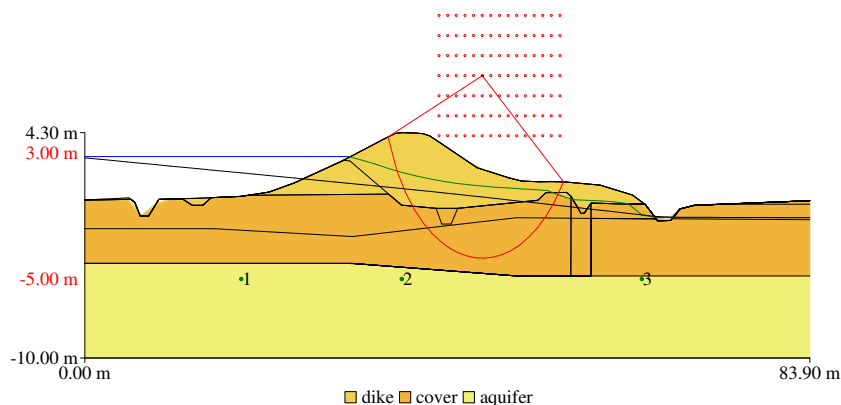


Figure 2: Slip circle.

discharge q_i (m/s). This expression reads

$$q_i = -\frac{k_r \kappa_{ij}}{\mu} \left(\frac{\partial p}{\partial x_j} - \rho g_j \right) \quad (1)$$

where p (N/m²) denotes the pore pressure, g_j (m/s²) indicates the gravitational acceleration vector components, ρ (kg/m³) expresses the density of the fluid, μ (kg m/s²) is the dynamic viscosity of the liquid phase, κ_{ij} (m²) indicate the components of the intrinsic permeability tensor of the soil skeleton, and k_r expresses the relative permeability of the porous medium. The mass balance equation reads

$$n \frac{\partial S}{\partial t} + (\alpha + n\beta) \frac{\partial p}{\partial t} = -\frac{\partial q_i}{\partial x_i} + \bar{q} \quad (2)$$

where α (m²/N) is the compressibility of the soil skeleton, β (m²/N) denotes the compressibility of the pore water and \bar{q} (1/s) expresses a source term. Alternatively the compressibility of the soil skeleton can be written as $\alpha = 1/(\lambda + 2\nu)$, where λ (N/m²) and ν (N/m²) denote Lamé constants.

The governing equation for saturated groundwater flow follows from Darcy's relation (1) and the mass conservation equation (2) as

$$n \frac{\partial S}{\partial t} + (\alpha + n\beta) \frac{\partial \phi}{\partial t} = \frac{\partial}{\partial x_i} \left(K_{ij} \frac{\partial \phi}{\partial x_j} \right) + \bar{q} \quad (3)$$

This equation is known as the storage equation. The primary variable in the storage equation is the hydraulic head ϕ (m), which reads $\phi = p/(\rho g) + z$, where z (m) is the elevation level. The hydraulic conductivity K_{ij} (m/s) is expressed as $K_{ij} = k_r \kappa_{ij} \rho g / \mu$. Its value depends on both the fluid phase and solid phase properties. For saturated conditions the relative permeability is constant, $k_r = 1$. The numerical model that will be presented

in this section is based on a more convenient control-volume form of the mass balance equation, which is given by

$$\int_{\Omega} n \frac{\partial S}{\partial t} d\Omega + \int_{\Omega} (\alpha + n\beta) \frac{\partial \phi}{\partial t} d\Omega = - \int_{\Gamma} q_i n_i d\Gamma + \int_{\Omega} \bar{q} d\Omega \quad (4)$$

where $n_i (-)$ denotes the outward pointing normal to the boundary Γ .

Dupuit considers one-dimensional horizontal flow through high permeability aquifers and one-dimensional vertical flow through low permeability aquitards. Dupuit's approximation transforms the storage equation for a system of two aquifers and a single aquitard into

$$\begin{aligned} \int_{\Omega^*} n \frac{\partial \phi_1}{\partial t} d\Omega &= \int_{\Gamma^*} kD_1 \frac{\partial \phi_1}{\partial x} n_x d\Gamma + \int_{\Omega^*} \frac{\phi_2 - \phi_1}{c} d\Omega + \int_{\Omega^*} \bar{q}_1 d\Omega \\ \int_{\Omega^*} (\alpha + n\beta) \rho g D_2 \frac{\partial \phi_2}{\partial t} d\Omega &= \int_{\Gamma^*} kD_2 \frac{\partial \phi_2}{\partial x} n_x d\Gamma + \int_{\Omega^*} \frac{\phi_1 - \phi_2}{c} d\Omega + \int_{\Omega^*} \bar{q}_2 d\Omega \end{aligned} \quad (5)$$

where $kD = K_{xx}D$ (m^2/s) is the transmissivity of a high permeability layer, and $c = d/k_{yy}$ (s) is the hydraulic resistance of the low permeability layer that separates both high permeability layers. The implicit finite volume discretization for both lines of equation (5) reads

$$\begin{aligned} aL_i \frac{\phi_{i,j}^{n+1} - \phi_{i,j}^n}{\Delta t} &= kD_{i+1/2,j}^{n+1} \frac{\phi_{i+1,j}^{n+1} - \phi_{i,j}^{n+1}}{x_{i+1,j} - x_{i,j}} - kD_{i-1/2,j}^{n+1} \frac{\phi_{i,j}^{n+1} - \phi_{i-1,j}^{n+1}}{x_{i,j} - x_{i-1,j}} \\ &\quad + L_i \frac{\phi_{i,j+1}^{n+1} - \phi_{i,j}^{n+1}}{c_{i,j+1}^{n+1}} - L_i \frac{\phi_{i,j}^{n+1} - \phi_{i,j-1}^{n+1}}{c_{i,j-1}^{n+1}} + Q_i \end{aligned} \quad (6)$$

where the horizontal extent of a single cell is given by $L_i = (x_{i+1} - x_{i-1})/2$ and its height reads $D_i = z_i^t - z_i^b$, where z_i^t denotes the elevation level of the top of cell i and z_i^b is the elevation level of the bottom of this finite volume cell. A prescribed flux $Q_i > 0$ specifies a flux into the system, and will be used for the definition of boundary conditions.

The effective transmissibility of an aquifer follows from summing up the transmissibilities k_s of the sub-layers that form the aquifer weighted by their thickness d_s according to $kD = \sum k_s d_s$. The thickness of an unconfined aquifer follows from the difference in position of the water table and bottom of the the aquifer. The effective resistance of an aquitard follows from summing the hydraulic resistance of all its sublayers, given by the quotient of the thickness of its sub-layers and their hydraulic conductivity as $c = \sum d_s/k_s$. The storage term $a (-)$ in equation (6) equals the effective porosity in the case of an unconfined aquifer and reads $a = n_e$. For the case of a (semi) confined aquifer the storage term reads $a = (\alpha + n\beta) \rho g D$. The time dependent behavior of the water pressure in the aquitards is taken into account by introducing an extra unknown for these layers, and adding equations for the aquitards to the system of equations for the aquifers (6) given by

$$aL_i \frac{\phi_{i,j}^{n+1} - \phi_{i,j}^n}{\Delta t} = L_i \frac{\phi_{i,j+1}^{n+1} - \phi_{i,j}^{n+1}}{c_{i,j+1}^{n+1}} - L_i \frac{\phi_{i,j}^{n+1} - \phi_{i,j-1}^{n+1}}{c_{i,j-1}^{n+1}} \quad (7)$$

This expression includes the consolidation coefficient $c_v = (\alpha + n\beta) \rho g/k$, which simulates the dissipation of pore pressures. The generation of pore pressures will be added to the system next.

Boundary conditions apply to artificial boundary layer nodes according to

$$\xi_i L_i (\nu_i^{n+1} - \phi_{i,j}^{n+1}) = L_i \bar{q}_i \quad (8)$$

where ν_i (m) is an artificial head and ξ_i (1/s) denotes connectivity. This expression specifies the source term $Q_i = \xi_i L_i (\phi_{i,j}^{n+1} - \nu_i^{n+1})$ in equation (6) and facilitates the modeling of flow through the unsaturated zone in a simplified way.

Dirichlet boundary conditions prescribe the head at the river boundary and the polder boundary as $\nu_i = \bar{\phi}$ and $\bar{q}_i = 0$, the conductivity ξ_i is set to an arbitrary large value. The conditions apply to the vertical boundaries of the first confined aquifer, where the connectivity is replaced by a reciprocal resistance. The resistance at the river side models the flow behavior outside the model domain as $\xi_i L_i = kD/l^*$, where l^* relates to the position where the river cuts the confined aquifer. The polder resistance enables a reduction of the model size in the other direction.

Free outflow of groundwater is prescribed by seepage conditions. Figure 1 shows a seepage face at the inner crest of the dike. Seepage boundary conditions set the pressure equal to the atmospheric pressure along the boundary as long as the groundwater flows out of the flow domain. The condition for this situation reads $\nu_i = z_i$ if $\tilde{q}_i \leq 0$, and state a no-flow condition if the pressure is less than atmospheric pressure as $\bar{q}_i = 0$ for $\nu_i < z_i$. An iterative procedure detects the state of the seepage condition and adjusts the state when needed; if the head is prescribed and inflow occurs then a zero flux is enforced, if the flux is set to zero and the pressure exceeds the atmospheric pressure then the head, which relates to atmospheric conditions, is enforced.

Submerging conditions state a prescribed head at the bottom of the river and parts of the outer crest. The first state of this condition applies if the river level is above the submerged part of the flow boundary. Either outflow or inflow might occur according to $\nu_i = \bar{\phi}$ if $\bar{\phi} > z_i$. Flow through the unsaturated zone is accounted for by setting $\xi_i = k_i/h_i$, where k (m/s) is the saturated hydraulic conductivity and h (m) expresses the height of the unsaturated zone, which reads $h_i = z_i - \phi_i$. For boundary nodes located at the river surface level the pressure will be zero $\nu_i = z_i$, the flux then follows from $\tilde{q}_i = \xi_i (z_i - \phi_i)$, which equals the saturated permeability because of the definition of ξ . Non-linear (effective) material behavior may be accounted for by imposing a functional relation $k = k(h)$. However, the flux through the unsaturated zone increases linearly with increasing surface pressure for submerged nodes. If the condition of this first state is not met then seepage boundary conditions are imposed, adding two states for submerging conditions. The proposed flow model is not able to simulate the fully coupled water phase - soil phase behavior because the equilibrium equation, describing the deformation of the soil skeleton, is omitted. Loading of the water phase underneath the river bed due to water level changes is taken into account in a heuristic manner. According to this

approach, the load increment $\delta\sigma$ (N/m²) distributes over the liquid phase δp (N/m²) and the solid phase $\delta\sigma'$ (N/m²) according to

$$\delta p = \frac{\alpha}{\alpha + n\beta} \delta\sigma \quad \delta\sigma' = \frac{n\beta}{\alpha + n\beta} \delta\sigma \quad (9)$$

For each time step, the hydraulic head obtained in the previous time step is adjusted as $\phi^{n*} = \phi^n + \alpha\Delta h/(\alpha + n\beta)$, where Δh is the water level increase over the time step.

Uplift conditions apply to the shallow aquifer and simulate the displacement of the low permeability cover layer due to excess pore water pressures. The head is prescribed if flow into the storage zone underneath the cover layer occurs. This state reads $\phi_i = z_i^t + \gamma d_i/\rho g$ if $\tilde{q}_i \geq 0$, where γ (N/m³) denotes the unit weight of the soil. No flow conditions apply if the calculated hydraulic head is less than the position of the bottom of the cover layer and read $\bar{q}_i = 0$ for $(\phi_i - z_i) \rho g > \gamma d_i$. Uplift conditions generalize the seepage condition.

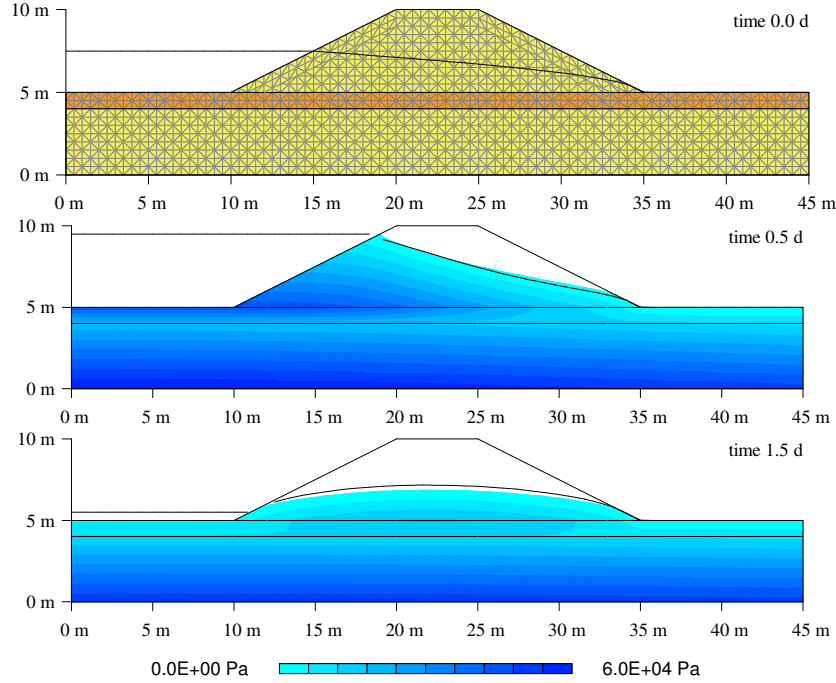


Figure 3: Water pressure fields.

Verification tests show that the results of the proposed Dupuit simulation compare well with the saturated/unsaturated flow simulation. Figure 3 presents an example where the calculated phreatic surface, which results from the proposed quasi two-dimensional simulation, is depicted as a line on top of the saturated pressure contours, which follow from the fully two-dimensional flow simulation. The embankment was loaded by varying river water level conditions according to $h = 7.5 + 2.0 \sin(\pi t)$, where t measures time in

days and h returns the river water level in meter. No-flow conditions apply to the left vertical boundary, a polder level of 5.0 m applies to the right vertical boundary. The reference simulation incorporates Van Genuchten material relations for saturation and relative permeability³. For the sandy material (aquifer and dike) the saturated parameters are given by $\kappa_{ij} = 9.44 \cdot 10^{-12} \text{ m}^2$, $\alpha = 10^{-8} \text{ m}^2/\text{N}$, $n = 0.287$, and unsaturated material behavior follows from $\psi_a = 0 \text{ m}$, $S_r = 0.01$, $S_s = 1$, $g_n = 2.286$, $g_a = 2.24$, $g_l = 0$. For the clay material (aquitard) the parameters read $\kappa_{ij} = 1.23 \cdot 10^{-14} \text{ m}^2$, $\alpha = 10^{-8} \text{ m}^2/\text{N}$, $n = 0.495$, $\psi_a = 0 \text{ m}$, $S_r = 0.01$, $S_s = 0.495$, $g_n = 1.525$, $g_a = 1.55$, $g_l = 0$.

3 Application

The proposed groundwater module is part of the dike analysis method (DAM) of the fluid early warning system (FEWS). This section illustrates the capability of the modeling tool by considering the stability response of the dike cross section depicted already in Figure 1 and Figure 2. FEWS provides a real time forecast of the hydrodynamic water level in the river, and returns an ensemble of 50 high water level scenarios. DAM assesses the stability of flood defense system by considering all scenario's. Figure 4 presents the high river predictions and the stability response for the cross section under consideration. The

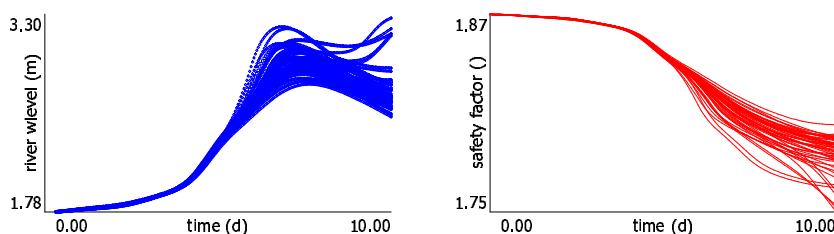


Figure 4: Predicted system behavior.

real time forecast of the safety of the flood defense system follows from a large number of cross section stability analyses, and the associated time-dependent pore pressure forecasts by groundwater flow simulation.

For this application groundwater flow calculations were carried out on a grid of 3 layers, each discretized by 100 cells, and 100 steps in time. The stability analysis used a grid of 100 center points each supporting 10 circles, resulting in 10^5 circle evaluations during the transient calculation of a single high water level realization. The coupled flow - stability calculation took about six seconds for a complete high water level scenario on a Intel core2 quad Q6600 2.40 GHz processor. The algorithm nearly scales linearly with the number of processors, using OpenMp parallelization, for an ensemble of high water level scenarios. The evaluation of the stability of an entire flood defense systems is distributed over multiple processors that do not share cross section information.

For the cross section under consideration monitoring data was not available yet. Here groundwater head observations are generated artificially to illustrate the modeling pro-

cedure. Figure 5 shows a measured high river signal, which is the actual realization over the previous forecasting period, and the related hydraulic head data collected in the first monitoring point (shown in Figure 1). This information is used for inverse modeling,

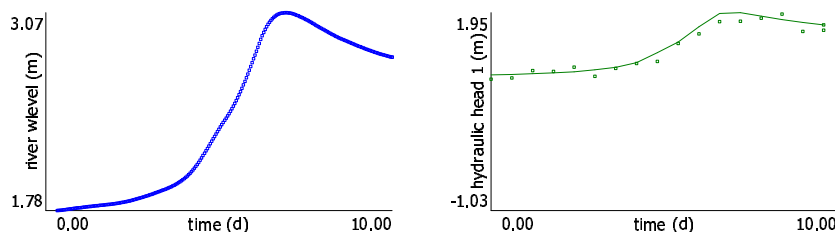


Figure 5: Observed system behavior.

which updates the geo-hydrological material behavior. The simulated final state of the system, based on these new river measurements and the material update, then provides a starting point for the next stability forecast.

4 Conclusions

The proposed method for modeling groundwater flow through dikes provides a computationally efficient procedure for predicting time dependent pore pressure fields in these constructions. The water pressure fields support a slope stability analysis for dike cross sections, which are successfully used for real time stability assessment of entire flood defense systems. The case study presented in this paper showed the stability response of a dike for a series of high water level scenarios. These results can be used to support decisions on timely preventive or remedial actions.

REFERENCES

- [1] R.B.J. Brinkgreve and R. Al-Khoury and J.M. van Esch. *Plaxflow*, Plaxis B.V. (2003).
- [2] G. de Marsily. *Quantitative Hydrogeology, Groundwater Hydrology for Engineers*, Academic Press, (1986).
- [3] J.M. van Esch. *Adaptive Multiscale Finite Element Method for Subsurface Flow Simulation*, PhD thesis, (2010).
- [4] W.H. Press and W.T. Vetterling and S.A. Teukolsky and B.P. Flannery. *Numerical recipes in C, The Art of Scientific Computing*, Cambridge University Press, (2002).
- [5] A. Verruijt. *Computational Geomechanics*, Kluwer Academic Publishers, (1995).
- [6] A.H. Weerts and J. Schellekens and F.S. Weiland. Real-Time Geospatial Data Handling and Forecasting: Examples From Delft-FEWS Forecasting Platform/System, *J. of Selected Topics in Applied Earth Observations and Remote Sensing*, (2010).